NATIONAL RADIO ASTRONOMY OBSERVATORY
SOCORRO, NEW MEXICO
VERY LARGE ARRAY PROGRAM

VLA SCIENTIFIC MEMORANDUM NO. 142

DESIGN CONSIDERATIONS FOR THE 327 MHZ FEED: THE EFFECT OF BEAM ELLIPTICITY ON DYNAMIC RANGE

Steven R. Spangler

April, 1982

I. INTRODUCTION

Crude calculations are sufficient to show that the sensitivity of the planned 327 MHz system for the VLA will be determined not by radiometer noise, but by "dynamic range noise" due to strong sources in the field. This fact should be kept in mind when designing the feed, which of course determines the single dish antenna pattern. For example, a uniform illumination of the reflector will maximize the forward gain, but it will also tend to enhance the sidelobe level and beam ellipticity. A heavily-tapered dish will have a reduced forward gain, but also a rounder beam and diminished sidelobes. It is not immediately obvious which antenna would have a higher Figure of Merit.

The purpose of this memo is to explore the effects of single dish beam ellipticity on the map noise level. The effect of beam ellipticity can be described quite simply. A source at some distance from the beam center will rotate through the beam pattern as the source is tracked. For an elliptical beam, the apparent flux density of the source will therefore change. The mapping process will interpret this variation as structure, and distribute the variable power over the map in a random fashion, thus raising the noise level. We now calculate the magnitude of this noise for different beam ellipticities.

II. APPARENT FLUX DENSITY VARIATIONS DUE TO AN ELLIPTICAL BEAM

We assume that all antennas in the array possess identical beam power patterns which can be described by an elliptical Gaussian function,

$$P(\theta_x, \theta_y) = \exp\left[-\left\{ (\theta_x/\Theta_x)^2 + (\theta_y/\Theta_y)^2 \right\}\right]. \qquad (1)$$

We now consider this antenna to be observing a source of unit flux density an angular density θ from the beam center at position angle χ. The geometry is shown in Figure 1.

In the worst case, the position angle χ will go from 0 to $\pi/2$ (and beyond) during the course of the observation. In this case, the maximum apparent flux density change of the source will occur, which we denote by δP. If P_1 is the apparent flux density when $\chi = \frac{\pi}{2}$, and P_2 is the same quantity when $\chi = 0$, we obviously have;

$$\delta P \equiv P_1 - P_2 = \exp\left[-(\theta^2/\Theta_x^2)\right] - \exp\left[-(\theta^2/\Theta_y^2)\right]. \qquad (2)$$

Denoting the beam ellipticity, ε, by;

$$\Theta_y = \varepsilon\,\Theta_x, \qquad 0 << \varepsilon \leq 1, \qquad (3)$$

and introducing a change of variables, $\xi \equiv \theta/\Theta_x$, we have:

$$\delta P = \exp[-\xi^2] - \exp[-\xi^2/\varepsilon^2]. \qquad (4)$$

This function has a maximum, ξ_{MAX}, at

$$\xi_{MAX} = \sqrt{\ln(1/\varepsilon^2)/[(1/\varepsilon^2 - 1)]} \qquad (5)$$

Values of ξ_{MAX} for some representative values of ε are given in Table 1 below.

TABLE 1

ε	ξ_{MAX}
0.95	0.97
0.90	0.96
0.80	0.89
0.70	0.83

The results of Table 1 show that the effect of beam ellipticity is maximized when a source is near the e^{-1} point of the beam.

Figure 2 shows plots of δP (solid lines, ordinate on left-hand side of plot) for values of ε =0.95,0.90,0.80, and 0.70. Figure 2 shows that the beam ellipticity effect is not trivial. If the beam ellipticity is 70%, a source located 80% of the way to the e^{-1} point (major axis) would contribute 25% of its flux for redistribution over the map. If the beam ellipticity is 90%, the same source would contribute about 7.5% of its flux for redistribution.

We now wish to estimate the flux density of sources which most probably will lie in this maximally vulnerable zone about one e^{-1} beamwidth from the field center. We consider sources stronger than a flux density S_0 . Such sources may be characterized by a mean solid angle per source, $<\Omega>$, which is just the inverse of the cumulative source count, i.e. $<\Omega> \propto S_0^{3/2}$. The normalized differential probability that the nearest such source lies an angle θ away from a random point on the sky is (Spangler, 1976, PASP,88,187)

$$P(\theta) = \frac{2\pi\theta}{<\Omega>} \exp\left[\frac{-\pi\theta^2}{<\Omega>}\right] . \qquad (6)$$

The probability density $P(\theta)$ is defined as the differential probability that the nearest source lies in an annulus of radius θ and width $d\theta$.

We now consider sources stronger than 1 flux unit at 327 MHz. From the low frequency source counts, we infer a mean solid angle per source, $\langle\Omega\rangle$, of 19072 arcmin^2. For the sake of simplicity, we assume that the 327 MHz beamwidth will conform to the VLA rule of thumb, FWHM = $1\overset{\prime}{.}5\lambda$(cm). It seems unlikely that the beamwidth will be that small, but a larger beamwidth would result in larger values for the dynamic range noise calculated below.

With the above assumptions, we can calculate the probability density, $P(\theta)$, which is plotted as a dashed line in Figure 2. The scale of the abscissa is the same as for the δP plots. The scale for the ordinate, shown on the right hand side of the plot, is normalized to the probability that the nearest source with flux density exceeding 1 Jy lies in an annulus of width equal to 10% of the e^{-1} beamwidth ($\sim$ 8.2 arcminutes) and radius indicated by the abscissa.

The results of Figure 2 may be summarized as follows. For the planned 327 MHz system, the probability will be $\geq$ 50% that a source with flux density $\geq$ 1 Jy will lie near the e^{-1} point of the beam where it will have the most serious effect on dynamic range. The gravity of the problem will depend strongly on the ellipticity of the beam. For example, if the ellipticity is of the order of 70%, we might expect 150 - 200 mJy to be available for mischief-making. If the ellipticity is 90%, this amount drops to 50 - 75 mJy.

III. RELATION BETWEEN δP AND THE MAP NOISE LEVEL

In the above section an expression was derived for δP, the change in the apparent flux density of a source due to beam ellipticity. Given the nature of the mapping process, this variation will be interpreted as structure, with the result that the variable flux will be "scattered" throughout the map and will be effectively noise. In this section, we will attempt to relate δP to the expected map noise level.

In the analysis, we envision a long synthesis observation (during which time the beam ellipticity effects become pronounced) as a set of snapshots. The "true" map, expressed as a series of snapshots is;

$$M_T(x,y) = \frac{1}{N} \sum_{i=1}^{N} S_i B_i(x,y) \quad . \tag{7}$$

Here x,y, are coordinates in the map plane, N is the number of snapshot maps averaged together, S_i is the apparent flux density of the contaminating point source at the time of the $i^{\underline{th}}$ snapshot, and $B_i(x,y)$ is the corresponding snapshot beam. The point-source-subtraction process will attempt to model the observed map by the following map;

$$M_M(x,y) = \frac{1}{N} \sum_{i=1}^{N} \bar{S} B_i(x,y), \tag{8}$$

where $\bar{S}$ is the average of S_i over the time of the synthesis. The point-source subtraction process will therefore leave a residual (noise) map, M_R , given by;

$$M_R(x,y) = \frac{1}{N} \sum_{i=1}^{N} (S_i - \bar{S}) B_i(x,y) \tag{9}$$

$$\text{or} \quad M_R(x,y) = \frac{1}{N} \sum_{i=1}^{N} f_i B_i(x,y),$$

where $f_i \equiv S_i - \bar{S}$. Obviously, $1/N \sum_{i=1}^{N} f_i = 0$.

Let us consider the residual map at a point x_1 , y_1 ,

$$M_R(x_1,y_1) = \frac{1}{N} \sum_{i=1}^{N} f_i B_i(x_1,y_1) \quad . \tag{10}$$

We expect that during the course of a synthesis observation the function $B_1(x_1,y_1)$ will resemble a pseudorandom function, characterized by an amplitude σ_b a correlation time scale τ , and an offset B_0 as shown below.

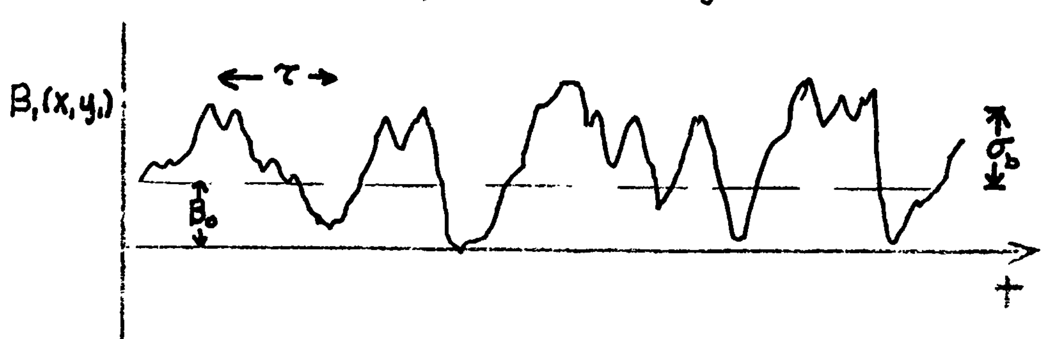

We model the beam by a "DC" term B_0 and a random, zero-mean component $b_i(x,y)$,

$$B_i(x,y) = B_0 + b_i(x,y).$$

The fact that f_i is zero mean implies that (10) may be rewritten as;

$$M_R(x_1,y_1) = \frac{1}{N}\sum_{i=1}^{N} f_i\, b_i(x_1,y_1). \qquad (11)$$

We now consider the sum $\sum f_i\, b_i(x_1,y_1)$. The function f_i changes on a time scale T, which is of the order of the duration of the observation. We now assume that $\tau \ll T$. In this case, there will have been many independent values of b_i during the time f_i has been ostensibly constant. We may therefore model the pixel value at (x_1, y_1) as a random walk with variable stepsize $f_i \sigma_b$. The probability distribution of the values of the sum $\sum_{i=1}^{N} f_i\, b_i(x_1,y_1)$ is then given by (Chandrasekhar in "Selected Topics in Noise and Stochastic Processes", N. Wax, ed.)

$$p(x,t) = \frac{1}{2\sqrt{\pi D t}} \exp\left[-\frac{x^2}{4Dt}\right], \qquad (12)$$

where D is the diffusion coefficient, $D = \frac{1}{2} n \langle \ell^2 \rangle$, $\langle \ell^2 \rangle$ being the mean-square stepsize, and n being the number of steps per unit time.

Clearly, $Dt = \frac{1}{2} N \langle \ell^2 \rangle$, where N is the total number of steps given above, and $\langle \ell^2 \rangle = \sigma_b^2 \langle f_i^2 \rangle$. The e^{-1} width of the probability distribution of the sum is then;

$$\sigma_s = \sqrt{2N\langle f_i^2\rangle}\,\sigma_b . \qquad (13)$$

The fact that this sum is normalized by the number of snapshots means that the rms noise level in residual map will be;

$$\sigma_M = \frac{\sqrt{2\langle f_i^2\rangle}\,\sigma_b}{\sqrt{N}} . \qquad (14)$$

The value of $\langle f_i^2 \rangle$ will depend on the details of the observations, but roughly $\sqrt{\langle f_i^2 \rangle} \sim f_{MAX}/\sqrt{2}$. In turn, $f_{MAX} = \frac{1}{2}\,\delta P S$ where S is the flux density of the contaminating source and δP is defined in section II above. With these assignments, equation (14) becomes;

$$\sigma_M = \frac{S\,\delta P\,\sigma_B}{2\sqrt{N}} \quad . \qquad (15)$$

Knowledge of σ_B requires a specific representation of the instantaneous beam. To this end, I used a dirty beam resulting from 3minutes of observation of 3C286. A grey-scale representation of the beam is shown in Figure 3. The observations were made at C band in the B array configuration. The map is 256x256 with a $0\overset{''}{.}4$ cell size. No taper was used, and (u,v) weighting was uniform. The default option in AIPS was used for the parameter UVBOX. The AIPS task IMEAN was run over a number of regions of the beam, and in each case resulted in a standard deviation of about 0.04. I have therefore used σ_B =0.05.

We now come to the important question of what estimate should be used for the number of snapshots, N. In the spirit of this calculation, we take it to be the number of independent values of the pseudorandom function $b_1(x,y)$ at the pixel (x_1, y_1). Figure 4 shows a contour plot of the beam in a random part of the field. From this Figure, we see that, roughly speaking, the angular diameter of the features is comparable to the synthesized beam shape of 1.6", at least in some directions. We shall therefore assume that the angular diameters of the beam features are comparable to the synthesized beam, θ . Now consider such a feature an angular distance Θ from the field center. As seen from the field center, this feature will subtend an angle Ω ,

$$\Omega = \theta/\Theta \quad . \qquad (16)$$

During the course of a 12 hour synthesis, the beam shown in Figure 3 will rotate through an angle of about π radians. The number N is therefore given approximately by;

$$N \simeq \frac{\pi \Theta}{\theta} = \pi N^{*}, \qquad (17)$$

where N^{*} is the distance to the feature in synthesized beams. We now have all the ingredients to compute the expected map noise level. In equation (15) I have used S= 1Jy, since in Section II it was shown that there is about a 50% probability that a source of 1 Jy or greater will be near the e^{-1} point of the primary beam where it can do the most damage. For δP I have chosen the maximum value, given a certain beam ellipticity, from Figure 2. As mentioned above σ_{g} has been set equal to 0.05. Finally, equation (17) has been used for N.

The results are shown in graphical form in Figure 5. The map noise level has been plotted against the distance N^{*} for several different values of the primary beam ellipticity ε . The plot shows the expected result that the beam ellipticity noise is larger near the contaminating source. Close to the contaminant, the rms noise ranges from 1.1 mJy/beam for an ellipticity of 70%, to less than 0.2 mJy/beam for an ellipticity of 95 %. The horizontal dashed lines indicate the expected noise level in a 12 hr integration for different bandwidths.

In view of the approximations made in obtaining our results, it is not clear how literally one should take the implications of Figure 5. It would seem, however, that unless severely constricted bandwidths must be used (due to interference), a primary beam ellipticity of less than 95 % would result in the map noise being dominated by dynamic range effects.

IV. SCALING OF RESULTS TO OTHER VLA BANDS

The effects discussed in this memo will occur at any frequency, and so it is therefore of interest to scale the results to the other VLA bands. First of all, the δP versus ξ curves shown in Figure 2 are valid for any frequency. Thus, the dimensionless distance ξ_{MAX} at which δP assumes its maximum value is a function only of the beam ellipticity. Since $\xi \equiv \frac{\theta}{\theta_0}$, and $\theta_0 \propto \nu^{-1}$, we obviously have $\theta_{MAX} \propto \nu^{-1}$, where θ_{MAX} is the angle at which δP is a maximum. We now contend that the greatest damage to dynamic range will be done by those sources whose $P(\theta)$ relationship maximizes at θ_{MAX}. The probability density (6) maximizes at an angle;

$$\theta'_{MAX} = \sqrt{<\Omega>/2\pi} . \qquad (18)$$

If we equate θ_{MAX} with θ'_{MAX}, we have;

$$<\Omega> \propto \theta'^{2}_{MAX} = \theta^{2}_{MAX} \propto \nu^{-2}. \qquad (19)$$

Thus the mean solid angle of the "most offending" sources is inversely proportional to the square of the frequency. We next are interested in the strength of these sources. We have seen above that, if S_0 represents the lower bound to the flux density of these sources, then;

$$<\Omega> \propto S_0^{3/2} \qquad (20)$$

so,

$$S_0 \propto <\Omega>^{2/3} \propto \nu^{-4/3}. \qquad (21)$$

Equations (20) and (21) make the assumption that the same sources which dominate the source counts at 327 MHz also dominate the counts at the frequency ν . For most of the VLA bands this assumption is incorrect. Counts at frequencies of about 1.4 GHz and below are dominated by steep spectrum sources, wheras at 5 GHz and above, flat spectrum sources make an increasing contribution to the counts. Nonetheless, we will continue this analysis with the understanding that the resultant flux densities will be lower limits. Equation (21) gives the 327 MHz flux densities of the sources responsible for contamination. We are naturally interested in the flux densities at the frequency of observation, which results (very roughly) in an additional factor of

$\nu^{-2/3}$. We therefore have;

$$S_0 \propto \nu^{-2} \qquad (22)$$

for the most contaminating sources. Since the flux density of the "worst offender" sources is $\propto \nu^{-2}$, it seems reasonable to conclude that the dynamic range noise estimates will also scale by this factor.

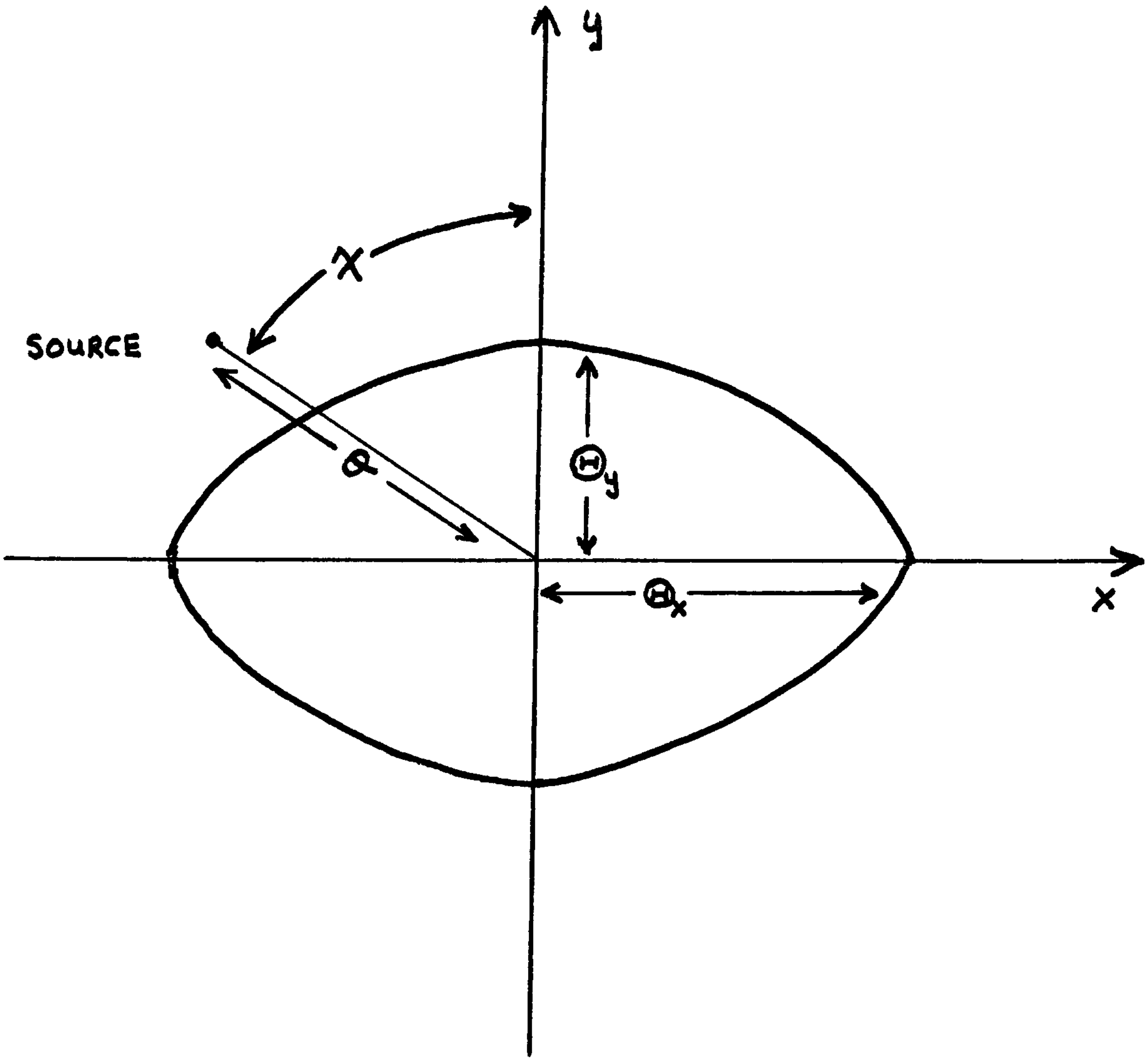

FIGURE 1

K+E 10 X 10 TO THE INCH • 7 X 10 INCHES KEUFFEL & ESSER CO. MADE IN U.S.A. 46 0780

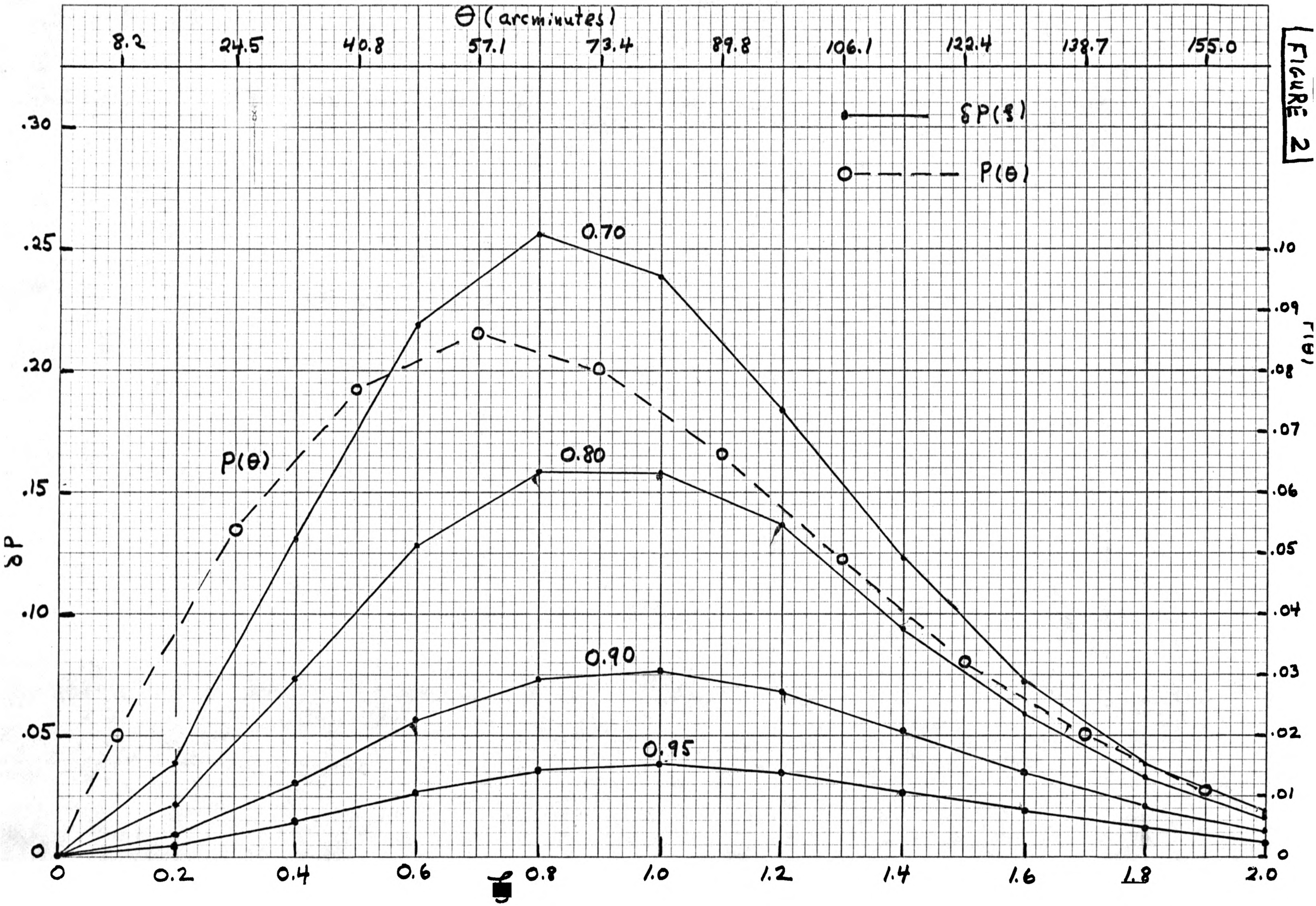

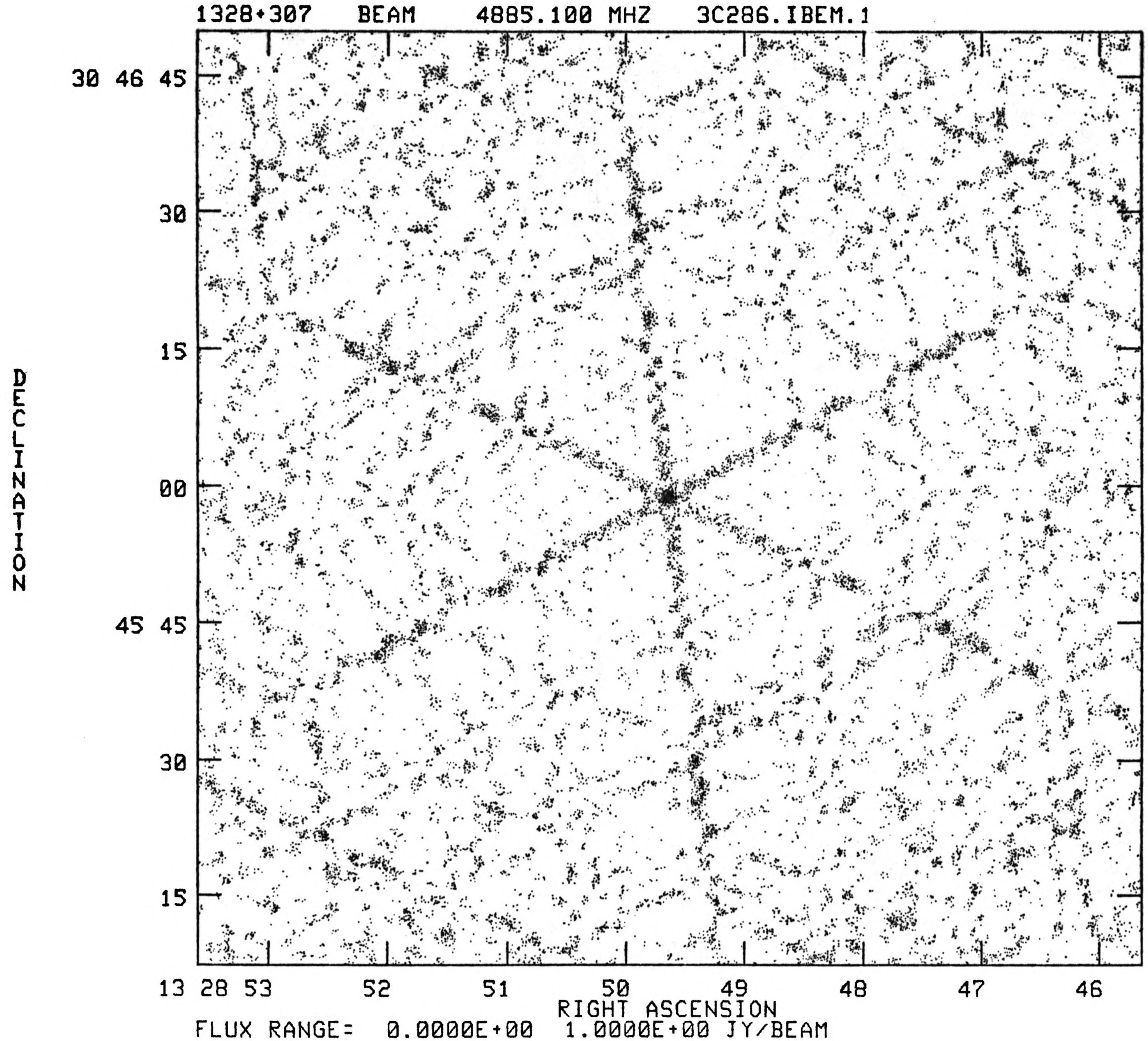
1328+307 BEAM 4885.100 MHZ 3C286.IBEM.1
DECLINATION
30 46 45
30
15
00
45 45
30
15
RIGHT ASCENSION
13 28 53
52
51
50
49
48
47
46
FLUX RANGE= 0.0000E+00 1.0000E+00 JY/BEAM

Figure 3

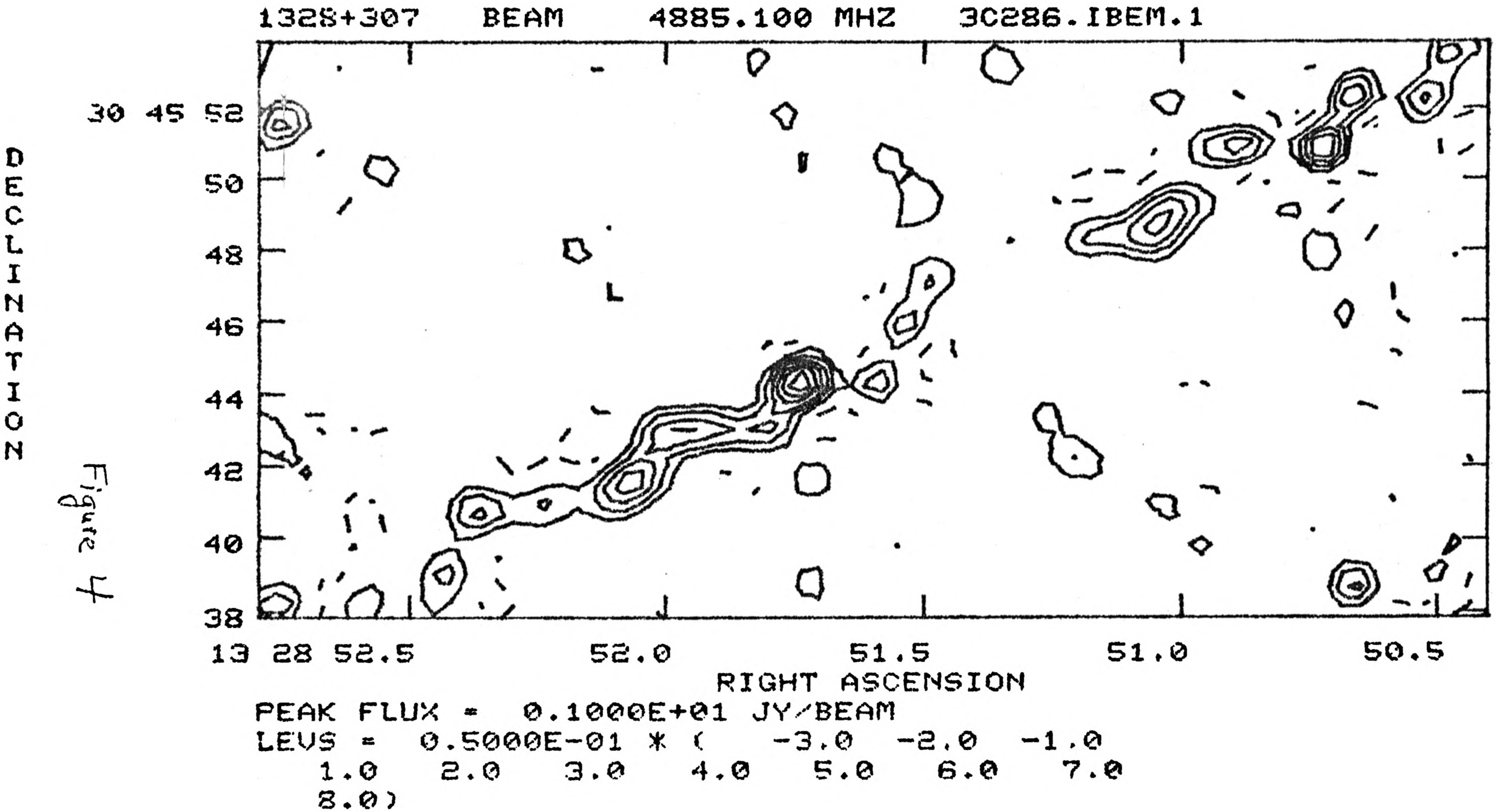
1328+307 BEAM 4885.100 MHZ 3C286.IBEM.1
DECLINATION
30 45 52
50
48
46
44
42
40
38
13 28 52.5
52.0
51.5
51.0
50.5
RIGHT ASCENSION
PEAK FLUX = 0.1000E+01 JY/BEAM
LEVS = 0.5000E-01 * (-3.0 -2.0 -1.0
1.0 2.0 3.0 4.0 5.0 6.0 7.0
8.0)

Figure 4

Map Noise Level Due to Primary Beam Ellipticity

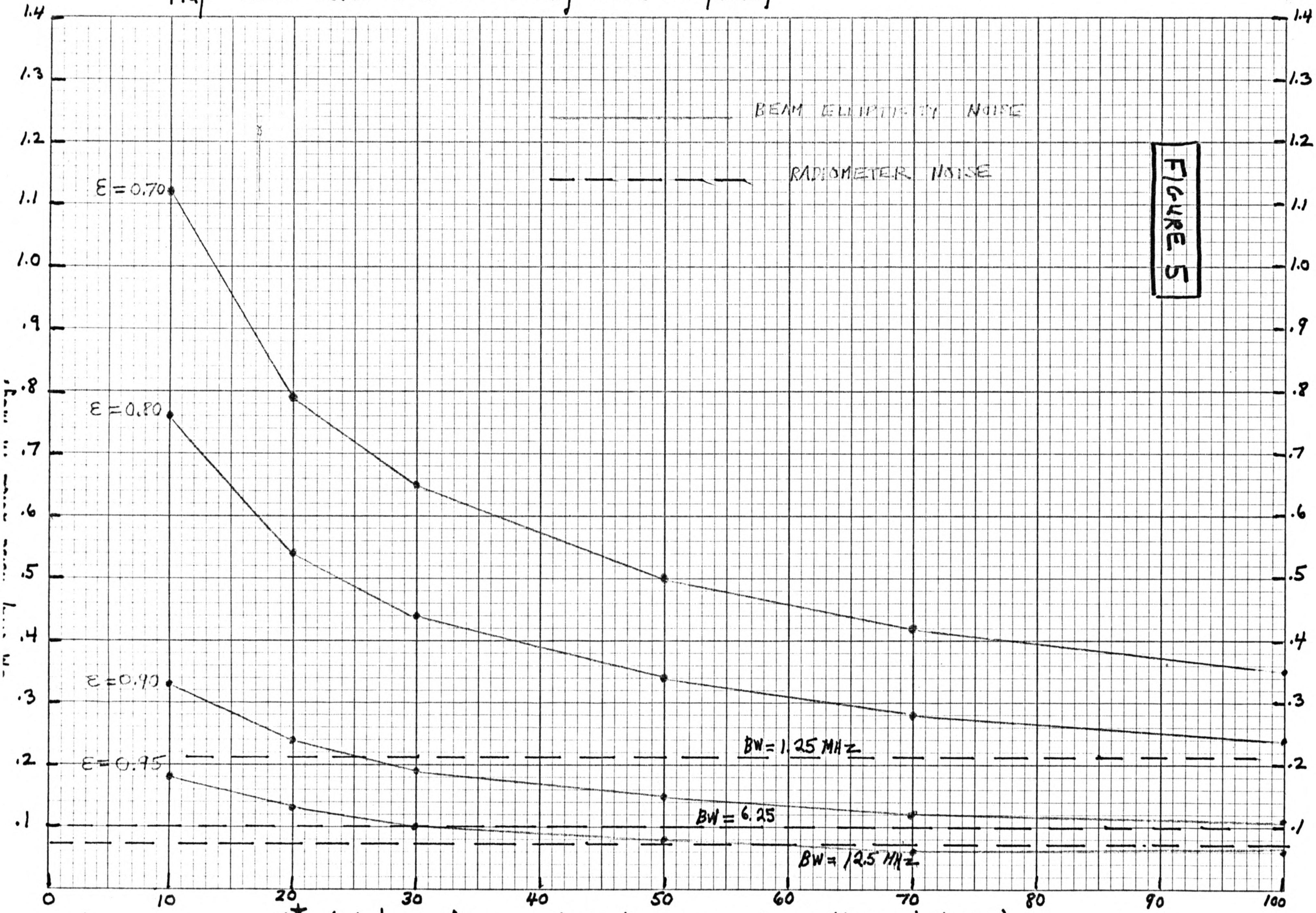

N^* (distance from contaminating source in synthesized beams)